Contribution from the Department of Chemistry,
Dartmouth College, Hanover, New Hampshire 03755

EPR Study of the Toluene Solution Properties of the Chromium(III)-Alkyl Complexes $[CpCrMeCl]_2$, $[Cp^*CrRCl]_2$ (R = Me, Et, CH_2SiMe_3), and $[Cp^*CrMeBr]_2$: Dimer-Monomer Equilibria in Solution

Joseph A. Barrera and Dean E. Wilcox*

Received September 12, 1991

EPR signals have been observed for a series of Cr(III)-alkyl complexes dissolved in toluene and the solution and frozen-solution EPR spectra have been used to characterize the structures and ground states of these complexes in solution. Both ligand (alkyl, halide) and metal (^{53}Cr) hyperfine splitting of these signals indicates that in the noncoordinating solvent toluene: CpCrMeCl exists entirely as a dinuclear complex, consistent with its dichloride-bridged solid-state X-ray structure; Cp*CrMeCl exists as an analogous dinuclear complex at higher concentrations but dissociates to a mononuclear structure upon dilution; Cp*CrEtCl and $Cp^*Cr(CH_2SiMe_3)Cl$ both exist entirely as monomeric coordinatively unsaturated structures; Cp*CrMeBr, though somewhat more complicated than the chloride complexes, exists in a dinuclear structure which appears to dissociate into a mononuclear species at low concentrations. Reactions of $[CpCrMeCl]_2$ or $[Cp^*CrMeCl]_2$ with trimethylphosphine or 4-*tert*-butylpyridine result in loss of the solution EPR spectrum and appearance of typical $S = {}^3/_2$ Cr(III) frozen-solution EPR signals, indicating formation of the three-legged piano stool adducts Cp(*)CrMeLCl. While the origin of the EPR signal from the antiferromagnetically coupled ground state of the dinuclear complexes has not been clearly established, the coordinatively unsaturated mononuclear complexes Cp*CrRCl (R = Me, Et, CH_2SiMe_3) have an $S = {}^1/_2$ ground state. The unprecedented large and well-resolved isotropic and anisotropic halide hyperfine coupling in these complexes suggests significant Cr(III)-Cl π bonding in a planar two-legged piano stool structure, which may be important in stabilizing these formally 13-electron complexes. Both increased steric properties of the Cp and alkyl ligands and decreased concentrations shift the dimer-monomer solution equilibrium toward the monomeric species; reactivity of the dichloride-bridged dinuclear molecules may be associated with these coordinatively unsaturated mononuclear complexes.

Introduction

There is a growing interest in paramagnetic organometallic complexes, in particular their reactivity,[1] compared to the reactivity of diamagnetic analogues, and their relevance to catalytic processes.[2] While NMR spectroscopy is not as generally useful in studying these molecules, EPR spectroscopy often can be used to characterize their electronic properties and provide new insight about their structure, bonding, and reactivity.

Recently Theopold and co-workers have prepared Cr(III)-alkyl complexes of the type $[CpCrRCl]_2$, where the crystal structure of $[CpCrMeCl]_2$ revealed[3a] a dichloride-bridged dinuclear structure, and solid-state magnetic data on this and related Cp* ($Cp^* = C_5Me_5^-$) complexes[3b] indicate an antiferromagnetic exchange coupling between two Cr(III) ions; they have used these complexes as an entry into novel organochromium reactivity, including olefin polymerization.[3c] We were interested in using these complexes to prepare paramagnetic heterodimetallic methylene-bridged molecules of the type $Cp_2\overline{TiCH_2MXL_2}$, analogous to diamagnetic complexes prepared by Grubbs and co-workers.[4] During the attempted synthesis of $Cp_2\overline{TiCH_2CrCl}MeCp^*$, however, $[Cp^*CrMeCl]_2$ did not react with the titanacycle $Cp_2\overline{TiCH_2CMe_2CH_2}$ under previously reported[4] conditions until the reaction mixture was diluted with toluene; this unexpected behavior led us to study the solution properties of $[Cp^*CrMeCl]_2$ and related Cr(III)-alkyl complexes.

Preliminary results showed that an EPR signal was associated with $[Cp^*CrMeCl]_2$ dissolved in toluene, thus allowing its solution properties to be investigated by this physical method. This led to a study, described herein, where EPR has been used to characterize the solution structural properties of the Cr(III)-alkyl complexes $[CpCrMeCl]_2$, $[Cp^*CrRCl]_2$ (R = Me, Et, CH_2SiMe_3), and $[Cp^*CrMeBr]_2$. Evidence is presented for equilibria in solution between the dimeric species and their formally 13-electron mononuclear complexes. Insight is also provided about the solution structure of the coordinatively unsaturated mononuclear Cr(III)-alkyl complexes.

Results

$[CpCrMeCl]_2$ (1). The EPR spectrum of a saturated toluene solution ($\sim 10^{-2}$ M) of the dinuclear Cr(III) complex[3a] $[CpCrMeCl]_2$ (**1**) is shown in Figure 1A. This spectrum exhibits hyperfine coupling with six equivalent protons from two methyl groups; however, a better fit to the experimental line width is obtained by also including hyperfine interaction with two equivalent chlorides. Figure 1B shows the best spectral simulation obtained with the parameters listed in Table I. Thus, the proton and chloride hyperfine coupling in the solution EPR spectrum of **1** indicate that a dimeric structure is retained in toluene, consistent with the crystal structure[3a] of this complex. In addition, the spectrum shows weak signals at higher and lower field which are due to those complexes with ^{53}Cr (9.45% abundance; $I = {}^3/_2$);[5] the magnitude of the isotropic chromium hyperfine constant (Table I) determined from these features is approximately half of that typical for mononuclear Cr(III) complexes[6] (see Table I) and consistent with a dinuclear[7] Cr(III) complex. Upon dilution of **1** to concentrations as low as 1×10^{-5} M there is no change in the solution EPR spectrum indicating that the dimeric structure of **1** is the predominant species at these concentrations in toluene. Figure 1C shows the 77 K frozen-toluene EPR spectrum of **1**,

(1) (a) Brown, T. L. *Ann. N.Y. Acad. Sci.* **1980**, *333*, 80-89. (b) Stiegerman, A. E.; Tyler, D. R. *Comments Inorg. Chem.* **1986**, *5*, 215-245. (c) Kowaleski, R. M.; Basolo, F.; Trogler, W. C.; Gedridge, R. W.; Newbound, T. D.; Ernst, R. D. *J. Am. Chem. Soc.* **1987**, *109*, 4860-4869. (d) Baker, R. T.; Calabrese, J. C.; Krusic, P. J.; Therien, M. J.; Trogler, W. C. *J. Am. Chem. Soc.* **1988**, *110*, 8392-8412.

(2) *Paramagnetic Organometallic Species in Activation/Selectivity, Catalysis*; Chanon, M., Julliard, M., Poite, J. C., Eds.; Kluwer Academic: Dordrecht, The Netherlands, 1989.

(3) (a) Richeson, D. S.; Hsu, S.; Fredd, N. H.; Van Duyne, G.; Theopold, K. H. *J. Am. Chem. Soc.* **1986**, *108*, 8273-8274. (b) Richeson, D. S.; Mitchell, J. F.; Theopold, K. H. *Organometallics* **1989**, *8*, 2570-2577; (c) Thomas, B. J.; Noh, S. K.; Schulte, G. K.; Sendlinger, S. C.; Theopold, K. H. *J. Am. Chem. Soc.* **1991**, *113*, 893-902.

(4) (a) Mackenzie, P. B.; Coots, R. J.; Grubbs, R. H. *Organometallics* **1989**, *8*, 8-14. (b) Ozawa, F.; Park, J. W.; Mackenzie, P. B.; Schaefer, W. P.; Henling, L. M.; Grubbs, R. H. *J. Am. Chem. Soc.* **1989**, *111*, 1319-1327.

(5) Statistical distribution of Cr isotopes in the dinuclear complexes gives $^{52}Cr^{52}Cr$, 81.8%; $^{52}Cr^{53}Cr$, 17.3%; and $^{53}Cr^{53}Cr$, 0.9%. Thus, these signals arise primarily from complexes with one ^{53}Cr.

(6) (a) McGarvey, B. M. *J. Chem. Phys.* **1964**, *41*, 3743-3758. (b) McGarvey, B. M. In *Transition Metal Chemistry*; Carlin, R. D., Ed.; Marcel Dekker: New York, 1967; Vol. 3, pp 89-201.

(7) This is true for $A(^{53}Cr) \ll J$ (the exchange coupling parameter), as is the case for these complexes; see: Kramer, S.; Clauss, A. W.; Francesconi, L. C.; Corbin, D. R.; Hendrickson, D. N.; Stucky, G. D. *Inorg. Chem.* **1981**, *20*, 2070-2077.

0020-1669/92/1331-1745$03.00/0

Table I. Experimental EPR Parameters

complex	g_{iso}[a]	$A_{iso}(^{1}H)$[a-c]	$A_{iso}(^{35,37}Cl)$[a-c]	$A_{iso}(^{53}Cr)$[b]	$A_{aniso}(^{35,37}Cl)$[b]
		A. Chromium Complex			
$[CpCrMeCl]_2$ (**1**)	1.996	16.34 (6)	1.0 (2)	23.7	
$[Cp^*CrMeCl]_2$ (**2**)	1.996	16.15 (6)	0.98 (2)	23.7	
$Cp^*CrMeCl$ (**3**)	1.992	12.91 (3)	2.65 (1)	44.6	18
$Cp^*CrEtCl$ (**8**)	1.9916	15.6 (2 α) 2.2 (3 β)	2.7 (1)	52.0	19.5
$Cp^*Cr(CH_2SiMe_3)Cl$ (**9**)[d]	1.9916	18.40 (2)	3.18 (1)	38.1	
$[Cp^*CrMeBr]_2$ (**10**)	1.996	16.12 (6)	0.56[f] (2)		
$Cp^*CrMeBr$ (**11**)	1.992	13 (3)	2.7[f] (1)		
$Cp^*CrMe(O)Cl$ (**12**)[e]	1.992	13.3 (3)	2.7 (1)	44.8	
		B. Cr^{+3} Doped Complex			
$AlCl_3 \cdot 6H_2O$[g]	1.9766			51.0	
$Co(acac)_3$[h]	1.9802			50.1	
MgO[i]	1.9800			48.9	
t-$[CoCl_2(en)_2]Cl \cdot HCl \cdot 2H_2O$[j]	1.9765			49.5	
$[Co(en)_3]Cl_3 \cdot NaCl \cdot 6H_2O$[j]	1.9874			48.6	
$(NH_4)_2[InCl_5(H_2O)]$[k]	1.9842			44.8	
MgS[l]	1.9874			45.9	
$K_3[Co(CN)_6]$[m]	1.992			44.1	

[a] Value obtained from simulation with 1.1 G line width, except where indicated. [b] Absolute value of hyperfine coupling in units of MHz. [c] Number of equivalent nuclei indicated in parentheses. [d] Simulation with 2.1-G line width. [e] Simulation with 2.7-G line width. [f] $A_{iso}(^{79,81}Br)$. [g] Wong, E. Y. *J. Chem. Phys.* **1960**, *32*, 598–600. [h] McGarvey, B. M. *J. Chem. Phys.* **1964**, *40*, 809–812. [i] Low, W. *Phys. Rev.* **1957**, *105*, 801–805. [j] Reference 6a. [k] Garrett, B. B.; DeArmond, K.; Gutowski, H. S. *J. Chem. Phys.* **1966**, *44*, 3393–3399. [l] Auzins, P.; Orton, J. W.; Wertz, J. E. In *Paramagnetic Resonance*; Low, W., Ed.; Academic: New York, 1963; Vol. 1, p 90. [m] Baker, J. M.; Bleaney, B.; Bowers, K. D. *Proc. Phys. Soc., London, Sect B* **1956**, *69*, 1205–1215.

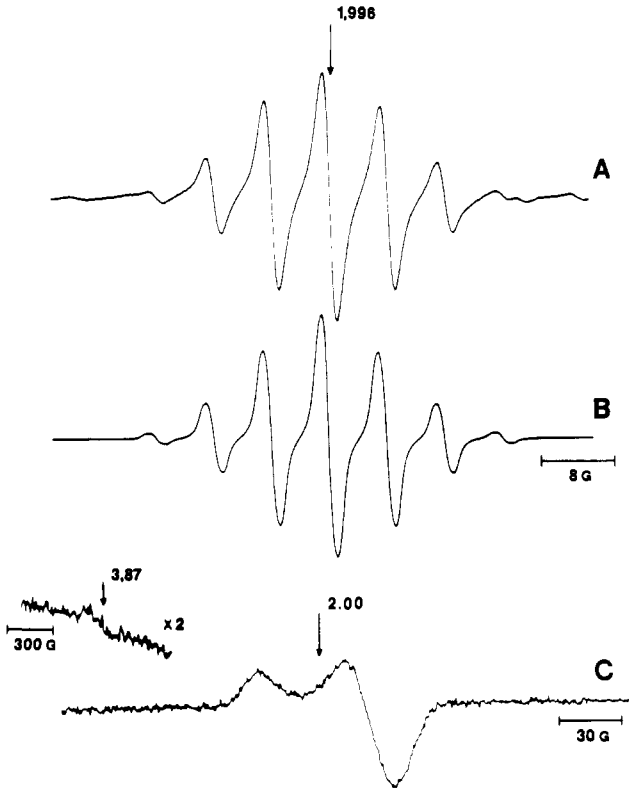

Figure 1. EPR spectra of $[CpCrMeCl]_2$: (A) toluene solution at 205 K; (B) simulation of A (see Table I for parameters); (C) frozen toluene solution of sample in A, 77 K.

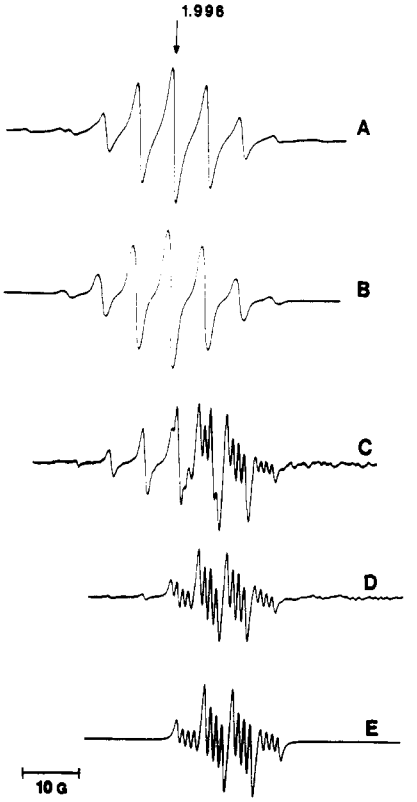

Figure 2. Solution EPR spectra of $[Cp^*CrMeCl]_2$ in toluene at 205 K: (A) $[Cr]_{total} = 8 \times 10^{-2}$ M; (B) simulation of A (see Table I for parameters); (C) $[Cr]_{total} = 8 \times 10^{-3}$ M (dilution of sample in A); (D) $[Cr]_{total} = 1 \times 10^{-4}$ M (dilution of sample in C); (E) simulation of D (see Table I for parameters).

which consists of features at $g = 2.022$ and 1.989 and a very weak feature at $g = 3.87$; this signal is not typical for six-coordinate Cr(III).[6,8]

$[Cp^*CrMeCl]_2$ (2). The EPR spectrum of an 8×10^{-2} M toluene solution of the dinuclear Cr(III) complex[3b] $[Cp^*CrMeCl]_2$ (**2**) is shown in Figure 2A. This EPR signal is nearly identical to that of **1** and can be simulated (Figure 2B) with hyperfine coupling from six equivalent protons and two equivalent chlorides using the parameters indicated in Table I. The magnitude of the ^{53}Cr hyperfine constant also supports a dinuclear[7] structure. Thus, at this concentration in toluene the EPR data for **2** are consistent with a structure similar to that of **1**. However, dilution of this sample to $[Cr]_{total} = 8 \times 10^{-3}$ M (Figure 2C) leads to the appearance of sharp new features with a smaller g value and further dilution to $[Cr]_{total} \leq 1 \times 10^{-4}$ M results in replacement of the EPR signal observed at higher concentration with that shown in

(8) (a) Hempel, J. C.; Morgan, L. O.; Lewis, W. B. *Inorg. Chem.* **1970**, *9*, 2064–2072. (b) Petersen, E.; Toftlund, H. *Inorg. Chem.* **1974**, *13*, 1603–1612. (c) Petersen, E.; Kallesoe, S. *Inorg. Chem.* **1975**, *14*, 85–88.

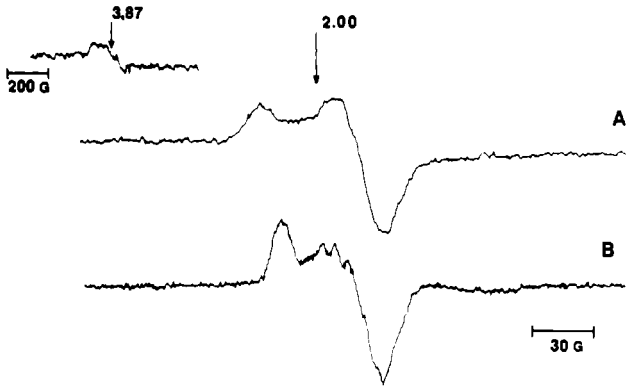

Figure 3. Frozen toluene solution (77 K) EPR spectra of $[Cp^*CrMeCl]_2$: (A) saturated solution; (B) $[Cr]_{total} = 5 \times 10^{-4}$ M (dilution of sample in A).

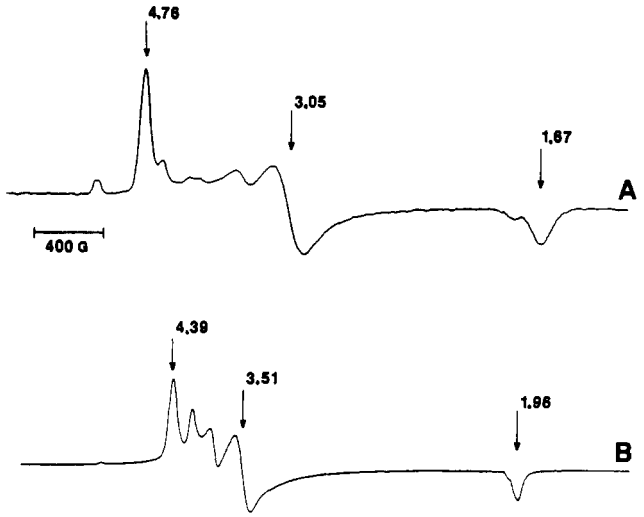

Figure 4. Frozen toluene solution (77 K) EPR spectra: (A) the reaction product of $[CpCrMeCl]_2$ and 1.2 equiv of PMe_3; (B) the reaction product of $[Cp^*CrMeCl]_2$ and excess 4-*tert*-butylpyridine.

Figure 2D. Simulation of this signal can only be achieved with hyperfine coupling to three equivalent protons and, surprisingly, with well-resolved hyperfine splitting from one chloride; parameters used in the best simulation (Figure 2E) are indicated in Table I. In addition, this spectrum (Figure 2D) shows a ^{53}Cr hyperfine value (Table I) which is in the range expected for mononuclear Cr(III).[6] This new EPR spectrum thus indicates the formation of the coordinatively unsaturated mononuclear complex $Cp^*CrMeCl$ (**3**) at low concentrations of **2** in toluene.

If a toluene solution of **2**, which exhibits the EPR signals assigned to **2** and **3** (Figure 2C), is concentrated by removing solvent under reduced pressure, there is an increase in the integrated intensity[9] of the EPR signal of **2** relative to that of the total EPR signal. Diluting this solution results in a decrease in the signal of **2** relative to the total EPR signal. These results indicate that in toluene there is a *reversible* concentration dependent equilibrium between the dimer **2** and the monomeric complex **3**.

Consistent with the similarity of the solution EPR spectra of **1** and **2**, the 77 K frozen-toluene EPR spectrum of a saturated solution of **2** (Figure 3A) is nearly identical to that of **1** (Figure 1C), including the weak feature at $g = 3.87$. However, under dilute conditions, where only the EPR signal of **3** is observed in solution, the 77 K EPR spectrum (Figure 3B) now shows signals at $g = 2.010$ and 1.986 and anisotropic chloride hyperfine splitting.[10] The absence of strong features in the $g = 4$ region

(9) A low-field portion of the signal from **2**, which does not overlap with that of **3**, was double integrated.

(10) This anisotropic hyperfine coupling is unambiguously due to the chloride since it is observed for both the methyl and the ethyl derivatives, which have different proton hyperfine splittings.

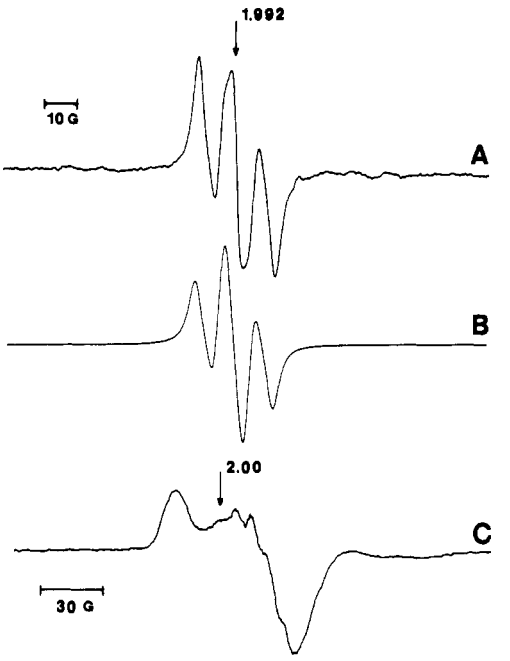

Figure 5. EPR spectra of $[Cp^*CrEtCl]_2$: (A) saturated toluene solution at 205 K; (B) simulation of A (see Table I for parameters); (C) frozen toluene solution of sample in A, 77 K.

indicates that **3** also is not a typical six-coordinate $S = {}^3/_2$ Cr(III) complex.[6,8]

Reactions of 1 and 2 with Nucleophiles. Both **1** and **2** react with nucleophiles, and it has been proposed[3a,b] that mononuclear adducts with three-legged piano stool structures are formed. Addition of 1.2 equiv of PMe_3 to a toluene solution of **1** (Figure 1A) results in loss of the solution EPR spectrum. The 77 K frozen-toluene EPR spectrum (Figure 4A), however, now exhibits prominent features at $g = 4.76$, 3.05, and 1.87, which are characteristic of a six-coordinate mononuclear Cr(III)[6,8] and are ascribed to $CpCrMeCl(PMe_3)$ (**4**); this complex is similar to the previously reported[3a] complex $CpCrMeCl(PPh_3)$. Qualitatively similar behavior is observed for the reaction of **2** with PMe_3; however, a 5-fold excess of phosphine is required to eliminate the solution EPR signal of **2**. The 77 K frozen-toluene EPR spectrum (not shown) now has prominent features centered at $g = 3.91$, ascribed to the PMe_3 adduct $Cp^*CrMeCl(PMe_3)$ (**5**).

Addition of excess 4-*tert*-butylpyridine to a toluene solution of **2** (Figure 2A) also results in complete loss of the solution EPR spectrum; the 77 K frozen-toluene EPR spectrum (Figure 4B) now shows strong features in the $g = 3.5$–4.5 region and a weaker associated feature at $g = 1.96$. This spectrum again indicates the formation of a six-coordinate Cr(III) complex,[6,8] assigned as $Cp^*CrMeCl$(4-*tert*-butylpyridine) (**6**), which appears to be consistent with the previously reported[3b] pyridine adduct of **2**.

$[Cp^*CrEtCl]_2$ (7). To investigate the effect of the alkyl ligand on the dimer–monomer equilibrium, the ethyl analogue of **2**, $[Cp^*CrEtCl]_2$ (**7**), was studied. Magnetic susceptibility measurements on **7** have indicated[3b] a dimeric structure in the solid state. The EPR spectrum of a saturated toluene solution of **7** is shown in Figure 5A; upon dilution this spectrum is unchanged except for a small variation in line width. While the spectrum is dominated by hyperfine coupling from two $I = {}^1/_2$ nuclei, it was not possible to achieve as good a simulation (Figure 5B) for this spectrum as was possible for the other solution spectra. The best interpretation (Table I) of this EPR signal assigns the dominant triplet splitting to the two α protons of a single ethyl ligand and the intensity pattern and line width to a combination of hyperfine coupling from the three ethyl β protons and a single chloride of a mononuclear complex; the isotropic ^{53}Cr hyperfine value (Table I) also is consistent with a mononuclear Cr(III) species. This suggests that the ethyl ligand, in conjunction with the more bulky Cp^*, shifts the dimer–monomer equilibrium in toluene entirely to the coordinatively unsaturated monomer

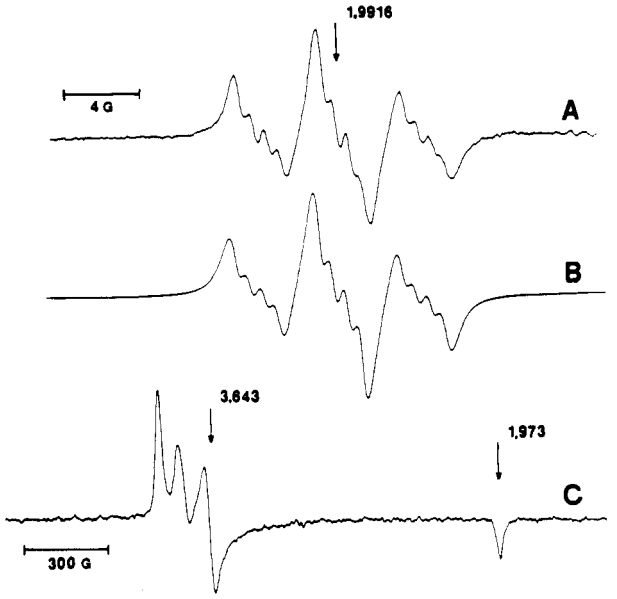

Figure 6. EPR spectra of $Cp^*Cr(CH_2SiMe_3)Cl$: (A) toluene solution at 205 K; (B) simulation of A (see Table I for parameters); (C) frozen toluene solution of sample in A, 77 K.

$Cp^*CrEtCl$ (**8**) under these conditions. The 77 K frozen-toluene EPR spectrum of **8** (Figure 5C) is very similar to that of **3** (Figure 3B), further supporting the mononuclear structure of this complex in toluene.

$Cp^*Cr(CH_2SiMe_3)Cl$ (9). To further explore the effect of the alkyl ligand the complex $Cp^*Cr(CH_2SiMe_3)Cl$ (**9**) was prepared. The EPR spectrum of a saturated toluene solution of **9** is shown in Figure 6A. This spectrum is unchanged upon dilution and can be simulated with hyperfine contributions from two equivalent protons and one chloride; the best simulation is shown in Figure 6B, and the simulation parameters are indicated in Table I. Thus, similar to the behavior of the ethyl derivative, the solution EPR data indicate that only the mononuclear species **9** exists in toluene. However, its 77 K frozen-toluene EPR spectrum (Figure 6C) surprisingly has strong features at $g = 3.5$–4.5 and an associated feature at $g = 1.973$, indicating that in frozen toluene this complex adopts a coordinatively saturated six-coordinate Cr(III) structure.[6,8] This was not observed for **3** and **8** in toluene and implicates the (trimethylsilyl)methyl ligand in completing the six-coordinate structure.

$[Cp^*CrMeBr]_2$ (10). To evaluate the contributions of the halide to the properties of **2**, the bromide analogue of **3**, which is expected to exist in the solid state as the dinuclear bromide-bridged complex $[Cp^*CrMeBr]_2$ (**10**), was prepared. Although we have not been able to obtain acceptable analytical analysis for this compound, a portion of the EPR spectrum of a 0.01 M toluene solution of **10** (Figure 7A) consists of a signal similar to that of **2**, which can be simulated (Table I) with hyperfine coupling to six equivalent protons and two equivalent bromides; however, a broad signal at $g = 2.01$ with poorly resolved hyperfine splitting also is observed. When the sample is diluted or warmed to 0 °C for 30 min, the broad $g = 2.01$ signal decreases and the signal associated with the dimeric species **10** increases (Figure 7B). This behavior and the breadth of the $g = 2.01$ signal suggests that it is primarily due to an oligomeric (or associated) species, where dipolar interaction between the paramagnetic centers leads to an increased relaxation rate and broadened line width; impurities that affect the analysis also could contribute to this signal. Figure 7C shows the EPR spectrum of a 5×10^{-4} M toluene solution of **10**; this exhibits, in addition to the signals seen in Figure 7B, sharp weak features at higher field that can be simulated with parameters (Table I) similar to those of **3**, suggesting the formation of $Cp^*CrMeBr$ (**11**) at low concentrations of **10**. While the solution properties of the bromide analogue of **2** are more complicated, the appearance at low concentration of weak signals very similar to those of **3** and attributed to a monomeric species suggests that

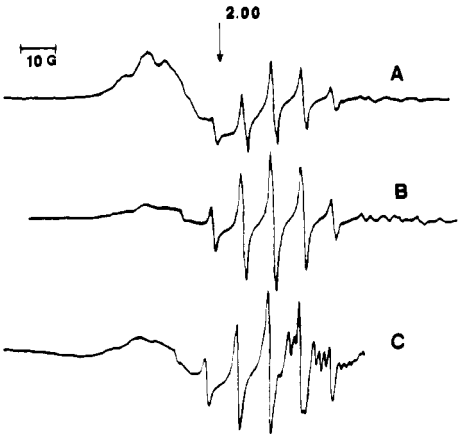

Figure 7. Solution EPR spectra of $Cp^*CrMeBr$ in toluene at 205 K: (A) $[Cr]_{total} = 1 \times 10^{-2}$ M (stirred at −30 °C for 30 min); (B) $[Cr]_{total} = 4 \times 10^{-3}$ M (dilution of sample in A); (C) $[Cr]_{total} = 5 \times 10^{-4}$ M (stirred at room temperature for 1 h).

the bromide complex also exists in an equilibrium between dimeric and monomeric structures. However, K_{eq} is estimated to be 2 orders of magnitude smaller than that of the analogous chloride complex.

Reactions of 2, 9, and 10 with O_2. Due to the rapid oxidation of these Cr(III)–alkyl complexes by dioxygen, reactions involving deliberate exposure to dry O_2 were undertaken to investigate the ERP spectra of the resulting oxidized species. A stream of O_2, dried by passage through a 2.5 × 30 cm column of Aquasorb (Malinkrodt), was passed for 15 s over a concentrated toluene solution of **2** which exhibited the Figure 2A EPR spectrum; the solution rapidly changed color from purple to green to red, the signal attributed to **2** was lost, and a new signal ~10 times more intense and exhibiting hyperfine coupling to three equivalent protons and a mononuclear $^{53}Cr(III)$ hyperfine value was observed. This EPR spectrum is attributed to an oxidized species, postulated to be the $S = {}^1/_2$ Cr(V) complex, $Cp^*CrMe(O)Cl$ (**12**), and is best simulated with the parameters in Table I. While this signal has an isotropic g value and hyperfine splitting similar to that of **3**, the magnitude of the proton hyperfine value (Table I) is quantitatively different and the line width is significantly broader,[11] such that the chloride hyperfine splitting is unresolved. Exposure of this solution to an additional 2 min of dry O_2, followed by 20 min of stirring at room temperature, converts this signal to one of similar intensity at $g = 1.988$ but lacking resolvable ligand hyperfine splitting; this signal also exhibits a ^{53}Cr hyperfine value (48.7 MHz) indicative of a mononuclear complex. A similar reaction of **9** with dry O_2 results in replacement of the Figure 6A EPR spectrum with a complicated signal dominated by a feature at $g = 1.9875$. Thus, these large spectral changes upon deliberate oxidation of **2** and **9** suggest that the EPR signals in Figures 2A,D and 6A do not originate from oxidized impurities.

The dioxygen reactivity of the bromide analogue **10** was studied also. When a stream of dry air is passed for 1 min over a sample exhibiting the EPR signal shown in Figure 7B, the purple solution begins to turn red, the signal due to **10** diminishes, and a broad feature at a higher g value begins to appear. Additional exposure to dry air for 20 min results in complete replacement of both the $g = 2.01$ feature and the $g = 1.996$ signal of **10** by a broad (~20 G peak-to-peak) unresolved spectrum at $g = 2.02$. Thus, the EPR signal attributed to **10** also does not appear to originate from an oxidized species.

Discussion

EPR spectroscopy has the potential to provide detailed information about the electronic and structural properties of paramagnetic complexes and has been used to characterize the ground state and bonding in Cr(III) molecules ranging from Werner

(11) The line width of this signal from the oxidized species **12** does not change upon dilution.

complexes[6,8] to the metallocenes.[12] In this study, EPR primarily has been used to characterize the solution structural properties of a series of Cr(III)–alkyl complexes originally prepared by Theopold and co-workers.[3a,b] This study also has provided new insight about the reactivity of these paramagnetic organometallic complexes.

Structure. The isotropic ^{1}H and $^{35,37}Cl$ hyperfine values required to simulate the solution EPR spectra of these Cr(III)–alkyl complexes and the magnitude of the observed isotropic ^{53}Cr hyperfine coupling show that at 205 K in toluene (1) CpCrMeCl exists entirely as a dimer, consistent with the solid-state X-ray structure,[3a] (2) Cp*CrMeCl exists in either a dimeric or monomeric structure depending on $[Cr]_{total}$, (3) Cp*CrEtCl and $Cp^*Cr(CH_2SiMe_3)Cl$ both exist entirely as monomeric coordinatively unsaturated structures, and (4) Cp*CrMeBr, though somewhat more complicated than the chloride complexes, exists in a dimeric structure which appears to dissociate into a mononuclear species at low concentration.

The anisotropic frozen-solution EPR spectra of these Cr(III)–alkyl complexes provide insight about their electronic ground states, which for **1**, **2**, **3**, and **8** are not typical of mononuclear six-coordinate Cr(III). The 77 K EPR spectra of **1** and **2** exhibit an anisotropic signal near $g = 2$ and a weak feature at $g = 3.87$. Since powder magnetic susceptibility data on these dinuclear complexes have been fit[3a,b] to an antiferromagnetically coupled pair of $S = {}^3/_2$ Cr(III) ions, the 77 K EPR signals of **1** and **2** originate from transitions within the Boltzmann populated $S = 1$, 2, and 3 spin states. Of these three, the $S = 1$ state has the highest thermal population, and the weak feature at $g = 3.87$ appears to be the forbidden half-field $\Delta M_s = \pm 2$ transition of the triplet state. However, EPR studies of antiferromagnetically coupled Cr(III) pairs[13] and high-symmetry dinuclear Cr(III) complexes[14] indicate that zero-field splitting of the $S = 1$ and $S = 3$ states generally is so large that allowed EPR transitions within these states are not observed at X-band frequencies. Thus, the anisotropic EPR signal near $g \approx 2$ (and the isotropic signal) of **1** and **2** may originate from the $S = 2$ state. Additional variable-temperature EPR measurements, currently underway, are needed to characterize further the ground state of these dinuclear complexes.

The 77 K EPR spectra of the mononuclear Cp*CrRCl complexes **3** (R = Me) and **8** (R = Et) lack the intense transitions in the $g = 4$ region expected for mononuclear $S = {}^3/_2$ Cr(III) and do not exhibit the weak $g = 3.87$ half-field transition of the dinuclear Cr(III) complexes; the observed signal in the $g = 2$ region indicates an effective $S = {}^1/_2$ ground state and a rhombic distortion from axial symmetry. $Cp^*Cr(CH_2SiMe_3)Cl$ (**9**) behaves somewhat differently, exhibiting a solution EPR signal (Figure 6A) similar to that of **3** and **8** but possessing a frozen-solution spectrum (Figure 6C) typical of a six-coordinate Cr(III) complex; the bulky (trimethylsilyl)methyl ligand is implicated in providing the coordinatively saturated frozen-solution structure. Addition of nucleophiles (L = PMe_3, 4-*tert*-butylpyridine) to **1** and **2** results in the species **4**–**6**, which exhibit 77 K EPR signals with $g_\perp \approx 4$ and $g_\parallel \approx 2$, characteristic of mononuclear six-coordinate Cr(III);[6,8] this supports the three-legged piano stool structure $Cp^{(*)}CrMeLCl$ for these complexes.

In spite of the inherent oxygen sensitivity of these Cr(III)–alkyl complexes, the observed EPR signals do not appear to originate from oxidized or impurity species on the basis of the following observations. The results reported here are consistently and quantitatively reproducible. Deliberate reaction of **2**, **9**, and **10** with dry dioxygen results in different EPR spectra, attributed to oxidized (Cr(V)) compounds. The solution structures of the Cr(III)–alkyl complexes, as determined by hyperfine coupling, are consistent with those expected on the basis of their characterization by other methods.[3a,b] Reactions of **1** and **2** with nucleophiles result in loss of the solution EPR signals and the appearance of frozen-solution EPR spectra typical of six-coordinate Cr(III), in agreement with the previously described chemistry.[3a,b]

To further confirm that the observed EPR signals do not originate from impurities, spin quantitation measurements, using the free radical spin standard DPPH, were made on **3**, which has a $S = {}^1/_2$ ground state analogous to the spin standard. We find that the integrated intensity of the EPR spectrum of a toluene solution of **2** with $[Cr]_{total} = 1 \times 10^{-4}$ M, which exhibits predominantly the EPR signal of **3** (Figure 2D), corresponds to only ~10% of the total Cr. While this might suggest that these EPR-detectable species are only a minor component, **3** is in equilibrium with the dimer **2**, which has a Boltzmann populated spin manifold and an EPR spectrum that appears to originate from the $S = 2$ state; since the quintet state of **2** has only 2.7% of the total dimer spin population at 205 K, based on the reported[3b] analysis of its powder magnetic properties, a large portion of **2** appears to be EPR-nondetectable, leading to the unexpectedly low concentration of **3** in the spin quantitation measurement. This is consistent with the ~10-fold increase in EPR signal intensity when **2** reacts with O_2 to give $S = {}^1/_2$ mononuclear Cr(V) species. To support this explanation further, we are able to reproduce the trend in relative EPR signal intensities of **2** and **3** in Figure 2A,C,D using an equilibrium concentration expression (see Experimental Section) and the assumption that the EPR signal of **2** arises from the thermally populated $S = 2$ spin state.

Bonding. The covalency of metal–ligand bonding in paramagnetic complexes can be evaluated from (1) the deviation of g values from 2.0023, which is due to spin–orbit coupling and reflects the amount of unpaired spin density on the metal, and (2) the magnitude of metal and ligand hyperfine values, which indicates the metal and ligand orbital contributions to the ground state. Both of these effects are readily apparent from the literature g values and ^{53}Cr hyperfine values collected in Table I, where it is observed that Cr(III) complexes with CN^- and S^{2-} exhibit larger g values and smaller $A(^{53}Cr)$ values relative to those found for similar complexes with O and N donor ligands. The data in Table I indicate that the Cr(III)–alkyl complexes studied here have an overall covalency comparable to that found for $Cr(CN)_6^{3-}$.

The EPR parameters of **1** and **2** (Table I) are very similar, indicating there is negligible change in the electronic structure and bonding in these complexes when Cp* is substituted for Cp. Comparison of the chloride complex **2** and the bromide complex **10** shows that the only major perturbation of the dinuclear Cr(III) electronic structure upon substitution of bromide for chloride is a decrease in the magnitude of halide hyperfine coupling. This decrease, though, indicates up to ~90% reduction[15] in unpaired spin density on the halide, suggesting reduced covalency in chromium bonding to the bridging bromides. This may correlate with the smaller dimer–monomer equilibrium constant of the bromide complex.

Major changes are observed, however, in the Cr(III)–alkyl electronic properties upon dissociation of **2** to **3** (Table I). The mononuclear complex exhibits a smaller isotropic g value (larger deviation from 2.0023) indicating a somewhat larger chromium contribution[16] to the ground state. The isotropic metal hyperfine coupling doubles in magnitude; however, this is primarily due to the 50% reduction of metal hyperfine coupling in dinuclear complexes,[7] and no major change is found upon dissociation when this is considered. The isotropic proton hyperfine coupling diminishes,

(12) (a) Ammeter, J. H. *J. Magn. Reson.* **1978**, *30*, 299–325. (b) Robbins, J. L.; Edelstein, N.; Spencer, B.; Smart, J. C. *J. Am. Chem. Soc.* **1982**, *104*, 1882–1893. (c) Castellani, M. P.; Geib, S. J.; Reingold, A. L.; Trogler, W. C. *Organometallics* **1987**, *6*, 1703–1712.

(13) (a) Henning, J. C. M.; van den Boef, J. H.; van Gorkom, G. G. P. *Phys. Rev. B* **1973**, *7*, 1825–1833. (b) Henning, J. C. M.; den Boom, H. *Phys. Rev. B* **1973**, *8*, 2255–2262. (c) McPherson, G. L.; Heung, W.; Barraza, J. J. *J. Am. Chem. Soc.* **1978**, *100*, 469–475. (d) McPherson, G. L.; Varga, J. A., Nodine, M. H. *Inorg. Chem.* **1979**, *18*, 2189–2195.

(14) (a) Beswick, J. R.; Dugdale, D. E. *J. Phys. C* **1973**, *6*, 3326–3340. (b) Benson, P. C.; Dugdale, D. E. *J. Phys. C* **1975**, *8*, 3872–3880. (c) Kremer, S. *Inorg. Chem.* **1985**, *24*, 887–890.

(15) This is based on the larger nuclear magnetic moment of bromide, although other factors affect the relative magnitude of the halide hyperfine splitting; see: Griffiths, J. H. E.; Owen, J. *Proc. R. Soc. London, A* **1954**, *236*, 96–111.

(16) Increased chloride contribution to the ground state would raise the g value.

Table II. Halide Spin Density

	% s(Cl)[a]	% π(Cl)[b]
A. Chromium Complex		
Cp*CrMeCl (3)	0.057	13.4
Cp*CrEtCl (8)	0.058	13.9
Cp*Cr(CH_2SiMe_3)Cl (9)	0.062	
B. Metal Ion Doped Complex		
Ir^{+4} in $(NH_4)_2[PtCl_6]$[c]		6.3
Mo^{+5} in $(NH_4)_2InCl_5 \cdot H_2O$[d]	e	6
Cr^{+3} in $KMgF_3$[f]	0.031[g]	4.76[g]

[a] Isotropic component. [b] Anisotropic component. [c] Griffiths, J. H. E.; Owen, J. *Proc. R. Soc. London, A* **1954**, *236*, 96–111. [d] Manoharan, P. T.; Rogers, M. T. *J. Chem. Phys.* **1968**, *49*, 5510–5519. [e] Isotropic hyperfine coupling unobserved. [f] Reference 17b; spin was normalized to an effective $S = {}^1/_2$ for comparison. [g] Fluoride.

suggesting a modest decrease in the covalency of Cr(III)–alkyl bonding. However, both qualitatively (Figure 2) and quantitatively (Table I) the most dramatic change is the 170% increase in the isotropic chloride hyperfine coupling, which indicates a considerable change in Cr(III)–chloride bonding in the coordinatively unsaturated mononuclear complex. To our knowledge, the magnitude and resolution of this isotropic chloride hyperfine is unprecedented in transition metal chemistry.

Isotropic ligand hyperfine coupling involves unpaired spin density with a finite probability at the ligand nucleus and arises from Fermi contact (direct spin transfer through σ bonding covalency with a ligand s orbital) and indirect spin polarization (π bonding covalency with ligand p orbitals resulting in spin polarization of ligand s electron density). Proton hyperfine coupling from alkyl ligands is obtained exclusively by the former mechanism. However, Fermi contact is expected to be small for halide ligands of O_h complexes with $(t_{2g})^3$ electronic configurations, and studies of Cr(III)-doped $KMgF_3$ indicate[17] that fluoride hyperfine coupling arises predominantly from π-bonding interaction through the indirect spin polarization mechanism. Although the mononuclear complexes Cp*CrRCl have an $S = {}^1/_2$ ground state, it would appear that the large increase in isotropic chloride hyperfine upon dissociation of **2** to **3** reflects an increase in Cr(III)–Cl π bonding in the coordinatively unsaturated monomeric complex.

Anisotropic ligand hyperfine coupling arises from both dipolar and bonding interaction. Considering the latter, halide anisotropic unpaired spin density for O_h Cr(III)–halide complexes is due primarily to π-bonding interaction, as indicated above. We have used the formalism developed by Stevens[18] to evaluate the ligand hyperfine coupling and quantify the ligand spin density as an estimate of the degree of covalency. Table II lists the isotropic (s) and anisotropic (π) chloride unpaired spin density of the mononuclear Cr(III)–alkyl complexes and other halide complexes. The values for the Cp*CrRCl complexes are found to be some of the largest ever observed, indicating significant π overlap between the Cr(III) and chloride. Thus, the large magnitude of anisotropic chloride hyperfine coupling in the coordinatively unsaturated mononuclear complexes also argues for a significant amount of Cr(III)–Cl π bonding[19] in these formally 13-electron complexes.

With few exceptions, Cr(III) molecules are six-coordinate. Thus, the structures of the coordinatively unsaturated Cp*CrRCl complexes in "non-coordinating" solvent are of considerable interest. Either a planar or a bent (pyramidal) two-legged piano stool structure is likely; 18-electron complexes such as $CpCo(CO)_2$ have the former structure, while an extended Hückel molecular

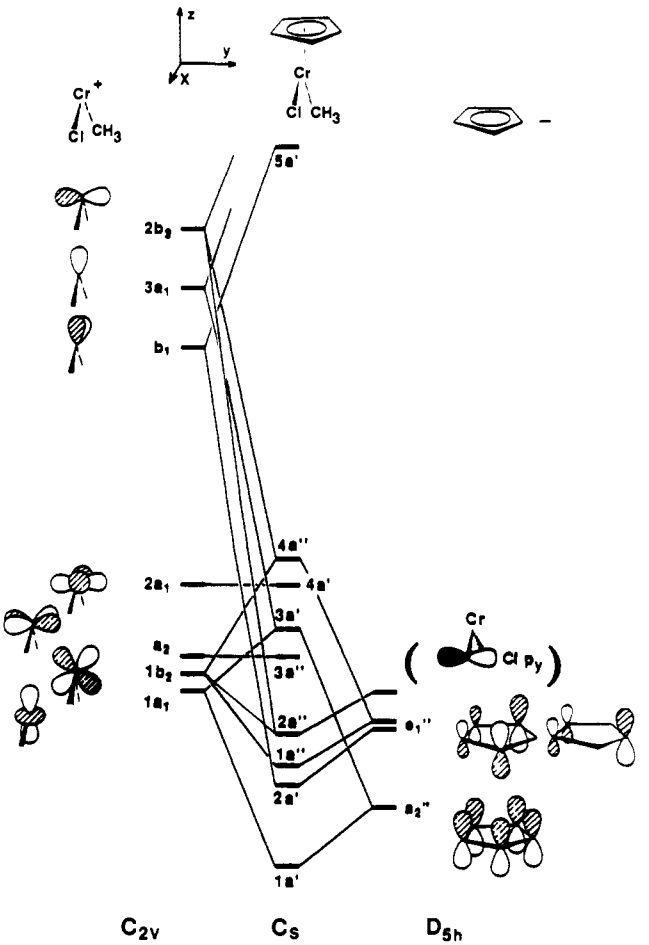

Figure 8. Qualitative molecular orbital diagram for the proposed planar structure of Cp*CrMeCl (3) with the chloride p_y orbital included and the effective symmetry indicated at the bottom. Adapted from ref 21.

orbital analysis of the 16-electron complex $CpMn(CO)_2$ suggests that the bent structure should be energetically favored.[20] To qualitatively evaluate the 13-electron complex Cp*CrMeCl, we consider a MO diagram (Figure 8) adapted from one[21] for the planar two-legged piano stool structure of $CpCo(CO)_2$. The chloride and methyl σ-bonding MO's are not included as they are much lower in energy; however, the filled chloride p_y orbital has been included. In this qualitative diagram the highest energy occupied and singly occupied molecular orbital (SOMO) is 3a', which is well separated in energy and thus consistent with the $S = {}^1/_2$ ground state indicated by the frozen-solution EPR data. The chloride p_y orbital has the correct symmetry and overlap to interact with the $1b_2$ (d_{yz}) and $2b_2$ (p_y) metal-centered orbitals, stabilizing the planar structure. Further, there also would be π interaction with the a_2 (d_{xy}) orbital which could place 3a'' higher in energy than 3a'; if this is the case, then the large observed chloride hyperfine would correlate with a direct halide π contribution to the SOMO 3a''.

The effect of pyramidalization on the total energy of Cp*CrMeCl is difficult to estimate. However, the good overlap between the chloride p_y orbital and the metal-centered orbitals in the planar structure would be diminished in a bent two-legged piano stool structure. This interaction allows for π donation to the electron-deficient Cr(III) and appears to correlate with the large experimentally observed chloride hyperfine coupling and support a planar two-legged piano stool structure. While a more quantitative analysis of the ground state and MO description of these coordinatively unsaturated Cp*CrRCl complexes is needed and currently is underway, these qualitative arguments are in

(17) (a) Helmholtz, L.; Guzzo, A. V.; Sanders, R. N. *J. Chem. Phys.* **1961**, *35*, 1349–1352. (b) Hall, T. P. P.; Hayes, W.; Stevenson, R. W. H.; Wilkens, J. *J. Chem. Phys.* **1963**, *38*, 1977–1984.
(18) (a) Stevens, K. W. H. *Proc. R. Soc. London, A* **1953**, *219*, 542–555. (b) Owen, J.; Thornley, J. H. M. *Rep. Prog. Phys.* **1966**, *29*, 675–728.
(19) Without additional electronic data it is not possible to exclude the possibility that an increase in σ bonding accompanies the change in molecular symmetry and contributes to the increase in chloride hyperfine.
(20) Hofmann, P. *Angew. Chem., Int. Ed. Engl.* **1977**, *16*, 536–537.
(21) Albright, T. A.; Burdett, J. K.; Whangbo, M. H. *Orbital Interactions in Chemistry*; Wiley: New York, 1985; pp 370–372.

agreement with the experimental data. Finally, we note that another series of recently prepared[22] d^3 complexes $CpMoX_2(PMe_3)_2$ (X = Cl, Br, I), which have four-legged piano stool structures, also have $S = {}^1/_2$ ground states like the coordinatively unsaturated Cp*CrRCl complexes; toluene solution EPR spectra of these 17-electron Mo(III) complexes exhibit phosphorus hyperfine coupling but halide hyperfine coupling is unresolved, preventing EPR characterization of the Mo(III)–halide bonding.

Reactivity. EPR data have indicated that in solution an equilibrium exists between the chloride-bridged dimer complex $[Cp^*CrMeCl]_2$ and the coordinatively unsaturated monomer Cp*CrMeCl. The concentration dependence of the EPR signals of **2** and **3** was used to estimate (see Experimental Section) that $K_{eq} \approx 1 \times 10^{-6}$ for the equilibrium $[Cp^*CrMeCl]_2 \rightleftarrows 2Cp^*CrMeCl$ at 205 K in toluene. For $[CpCrMeCl]_2$ the equilibrium constant must be at least 3 orders of magnitude smaller under similar conditions. Thus, the presence of Cp* destabilizes the dimeric structure by ≥12 kJ/mol relative to Cp. This behavior is very similar to that of $[CpCr(CO)_3]_2$, where the dimer–monomer equilibrium has been quantified by McLain.[23] The Cp* analogue of this complex also has been studied,[24] and as observed for the Cr(III)–alkyl complexes studied here, the more bulky Cp* shifts the equilibrium toward the monomeric species. However, in contrast to the Cr(III)–alkyl complexes, the resulting 17-electron mononuclear Cr(I)–carbonyl has a coordinatively saturated three-legged piano stool structure.

Reaction of the Cr(III)–alkyls with nucleophiles leads to formation of complexes that exhibit typical $S = {}^3/_2$ Cr(III) EPR signals, consistent with the proposed[3a,b] three-legged piano stool structures for these adducts. Six-coordinate Cr(III) complexes are substitutionally inert, suggesting that the ligand substitution reactivity of these Cr(III)–alkyl may be due to the coordinatively unsaturated 13-electron monomeric species observed to be in equilibrium with the coordinatively saturated chloride-bridged dimers in solution. One way to increase this reactivity, therefore, would be to increase ligand steric properties to disfavor the dimeric structure, as was found through comparison of analogous Cp and Cp* complexes and comparison of the methyl, ethyl, and (trimethylsilyl)methyl complexes. Theopold has used another strategy[3a] to enhance reactivity of the dinuclear chloride-bridged Cr(III)–alkyl complexes; treating with reagents such as Tl(I) salts, which abstract chloride, removes the bridging halide ligands and results in coordinatively unsaturated species which have been used to explore[3] the chemistry of these Cr(III)–alkyl complexes.

In solution, dinuclear molecules can dissociate into mononuclear species when their concentration is decreased; as observed here for the complexes $[Cp^*CrRX]_2$, this type of solution behavior may be more general than presently thought. This study has shown that EPR spectroscopy is an excellent method for studying the solution properties of Cr(III) organometallic complexes, in particular identifying dimer–monomer equilibria and characterizing the species involved.

Experimental Section

All operations were carried out in oven-dried glassware using standard Schlenk techniques under an atmosphere of dinitrogen purified by passage through columns of BASF R3-11 catalyst (Chemalog) and activated (350 °C for 3 days) 4-Å molecular sieves. Compounds were transferred and stored in a dinitrogen-filled Vacuum Atmospheres glovebox equipped with a HE-492 gas purification system and a −25 °C freezer.

EPR spectra were obtained with a Bruker ESP-300 EPR spectrometer using the following data collection parameters: 100 kHz modulation frequency, 0.08–0.5 G modulation amplitude, 82 ms time constant, 42 s sweep time, and three to nine scans; 0.3–1.0 mW microwave power was used (power saturation analysis[25] indicated negligible saturation of the solution EPR signals at this power setting). The microwave frequency was determined by a HP X532B frequency meter and the magnetic field was calibrated with DPPH ($g = 2.0037$). Unless otherwise noted, solution spectra were recorded at 205 K, using a Bruker ER 4111 variable-temperature unit, as this temperature gave the best resolved EPR signals; frozen-solution spectra were obtained with a Wilmad liquid-nitrogen EPR Dewar flask. EPR sample tubes were prepared from 4 and 2 mm i.d. Supersil quartz tubing (Heraus–Amersil). Simulations of solution EPR spectra were performed with software provided by Bruker, a Lorentzian line shape was used, and the line width parameter was fixed at 1.1 G, unless otherwise indicated, as this value gave the best simulation for the most highly resolved signal, that of **3** in toluene.

Typically samples for EPR measurements were prepared by adding ~15 mg of a solid sample to a small Schlenk flask in the glovebox and then adding ~3 mL of toluene at −25 °C and stirring for 20 min to ensure complete dissolution. An EPR tube was capped with a rubber septum, cooled to −60 °C, and purged several times with dinitrogen. A ~0.5-mL aliquot of the sample was then transferred into the EPR tube with a gastight syringe, and the syringe hole in the septum was covered with stopcock grease.

All solvents were distilled over drying agents under an atmosphere of dinitrogen: toluene and *n*-decane were distilled from Na; THF, diethyl ether, and pentane (in the presence of tetraglyme) were distilled from Na/K alloy and benzophenone; methylene chloride was distilled from P_4O_{10}. Anhydrous $CrCl_3$, PMe_3, $AlMe_3$, $Et_2Al(OEt)$, *n*-BuLi, $Cr(CO)_6$, Br_2, MeMgBr, and Me_3SiCH_2MgCl were obtained from Aldrich Chemical Co. and used without further purification. All lithium reagents were quantified by titration with diphenylacetic acid. TlCp (Aldrich) was purified by sublimation. 4-*tert*-butylpyridine (Aldrich) was stirred over CaH_2 overnight and then vacuum distilled into a round-bottom flask containing activated 4-Å molecular sieves (Linde). Microanalyses were performed by Spang Microanalytical Laboratory, Eagle Harbor, MI.

Literature methods were used to prepare the following compounds: $CrCl_3(THF)_3$,[26] Cp*H,[27] $RCrCl_2(THF)_3$ (R = Me, Et),[28] and $[Cp^*CrBr_2]_2$.[29] $[CpCrMeCl]_2$ (**1**) was synthesized from $MeCrCl_2(THF)_3$ and TlCp as previously reported[3a] and recrystallized from toluene at −80 °C to give red/purple cubelike crystals, which were isolated in 63% yield. $[Cp^*CrMeCl]_2$ (**2**) was synthesized from $MeCrCl_2(THF)_3$ and Cp*Li as previously reported[3b] and recrystallized from toluene at −80 °C to give a dark violet crystalline solid in 63% yield. (Anal. Calcd for $C_{11}H_{18}ClCr$: C, 55.61; H, 7.58; Cl, 14.92. Found: C, 54.84; H, 7.68; Cl, 15.15.) $[Cp^*CrEtCl]_2$ (**7**) was synthesized from $EtCrCl_2(THF)_3$ and Cp*Li as previously reported[3b] and recrystallized from toluene/pentane at −80 °C to yield a dark purple solid.

$Cp^*Cr(CH_2SiMe_3)Cl$ (9). $CrCl_3(THF)_3$ (0.82 g, 2.2 mmol) and Cp*Li (0.3 g, 2.1 mmol) were added to a 50-mL Schlenk flask in the glovebox. Cold THF (30 mL) at 0 °C was added to the ice-cooled flask, and the suspension was stirred for 5 min. The ice bath was removed, and the suspension was stirred for 90 min at room temperature. Me_3SiCH_2MgCl (1.0 M in Et_2O, 2.1 mL, 2.1 mmol) was added dropwise via syringe over a 5-min period at room temperature, during which time the solution changed color from azure to dark purple. The solution was stirred for 30 min and the THF was removed under reduced pressure at 0 °C. The purple/gray solid was extracted with a minimum of pentane, and the purple solution was placed in a −15 °C freezer for 2 days, followed by 7 days in a −80 °C freezer. The purple, flaky powder was isolated and dried under vacuum at 0 °C. Yield: 0.36 g, 40%. Anal. Calcd for $C_{14}H_{26}ClCrSi$: C, 54.26; H, 8.46. Found: C, 53.61; H, 8.77.

$[Cp^*CrMeBr]_2$ (10). $[Cp^*CrBr_2]_2$ (0.40 g, 1.15 mmol) was added to a 50-mL Schlenk flask in the glovebox. THF (25 mL) was added and the blue solution cooled to −50 °C. MeMgBr (1.5 M in toluene/THF, 0.85 mL, 1.3 mmol) was added dropwise with a syringe over a 10-min period. The solution slowly was warmed to −30 °C and stirred for 2 h. During this time the solution turned purple, after which the solution was stirred for 1 h at 0 °C, followed by 1 h at room temperature. The THF was removed under reduced pressure at 0 °C, to afford a violet/gray solid. This solid was extracted with toluene (1 × 12 mL and 1 × 6 mL) and the purple extracts were filtered over Celite. Additional toluene (2 × 4 mL) was used to extract the purple product from the filter. The toluene was partially removed under reduced pressure to a volume of ~15 mL at 0 °C. This solution was transferred with a filter cannula into a small Schlenk flask and placed in a −80 °C freezer for 4 days. A violet crystalline solid appeared, which was washed with cold pentane (3 × 1

(22) (a) Kreuger, S. T.; Poli, R.; Reingold, A. L.; Staley, D. L. *Inorg. Chem.* **1989**, *28*, 4599–4607. (b) Kreuger, S. T.; Owens, B. E.; Poli, R. *Inorg. Chem.* **1990**, *29*, 2001–2006.
(23) McLain, S. J. *J. Am. Chem. Soc.* **1988**, *110*, 643–644.
(24) Jaeger, T. J.; Baird, M. C. *Organometallics* **1988**, *7*, 2074–2076.
(25) Beinert, H.; Orme-Johnson, W. H. In *Magnetic Resonance in Biological Systems*; Ehrenberg, A., Malmström, B. G., Vänngård, T., Eds.; Pergamon: Oxford, England, 1967; pp 221–247.
(26) Manzer, L. E. *Inorg. Synth.* **1982**, *21*, 135–140.
(27) Manriquez, J. M.; Fagan, P. J.; Schertz, L. D.; Marks, T. J. *Inorg. Synth.* **1982**, *21*, 181–185.
(28) Nishimura, K.; Kuribayashi, H.; Yamamoto, A.; Ikeda, S. *J. Organomet. Chem.* **1972**, *37*, 317–329.
(29) Morse, D. B.; Rauchfuss, T. B.; Wilson, S. R. *J. Am. Chem. Soc.* **1988**, *110*, 8234–8235.

mL) at −60 °C and vacuum dried at 0 °C. Yield: 0.13 g, 40%. Anal. Calcd for $C_{11}H_{18}BrCr$: C, 46.86; H, 6.43; Br, 28.35. Found: C, 42.89; H, 5.92; Br, 26.68.

Determination of K_{eq} for the Equilibrium between 2 and 3. The value of K_{eq} for the equilibrium $[Cp^*CrMeCl]_2 \rightleftarrows 2[Cp^*CrMeCl]$ was estimated using the concentration dependence of the intensity of the characteristic EPR signal of **3** in Figure 2. For a simple dimer–monomer equilibrium, where $K_{eq} = [\mathbf{3}]^2/[\mathbf{2}]$ and $[Cr]_{total} = [\mathbf{3}] + 2[\mathbf{2}]$, it can be shown that solving for [**3**] and taking the real root gives the expression

$$[\mathbf{3}] = (1/4)K_{eq}(\{(8[Cr]_{total} + 1)/K_{eq}\}^{1/2} - 1) \quad (1)$$

Since the EPR signal of **3** is not observed in Figure 2A, this sets the limit that $[\mathbf{3}]/[Cr]_{total} < 0.01$ at $[Cr]_{total} = 8 \times 10^{-2}$ M. A value of $K_{eq} = 1 \times 10^{-6}$ gives $[\mathbf{3}]/[Cr]_{total} = 0.0025$, which is consistent with the absence of the monomer signal in Figure 2A. While **3** appears to have a $S = {}^1/_2$ ground state, the origin of the signal from **2** is not clear, making it difficult to compare quantitatively the two signal intensities. However, if the EPR signal of **2** arises from the thermally populated $S = 2$ state (antiferromagnetic coupling[3b]), then at 205 K for $K_{eq} = 1 \times 10^{-6}$ we calculate the signal intensity ratio, $I(\mathbf{3})/I(S = 2 \text{ of } \mathbf{2})$, to be 1/11, 1/3, and 3/1 for parts A, C, and D of Figure 2, respectively; this is the correct trend, with only the Figure 2D ratio appearing to be too small.

Acknowledgment. We are grateful to Robert Ditchfield and Russell Hughes for valuable discussions and thank Russell Hughes for the use of his glovebox. We thank one reviewer for drawing our attention to overlap between the chloride p_y and chromium d_{xy} orbitals in **3** and another for pointing out the relationship between monomer and total metal concentrations for a dimer–monomer equilibrium. The EPR spectrometer was purchased in part with funds from the National Science Foundation (Grant CHE 8701406) and the Dreyfus Foundation.

Contribution from the Departments of Chemistry and Physics, Rutgers University, New Brunswick, New Jersey 08903

Ligand Isomerism and Stacking in Square Planar Platinum(II) Complexes

M. J. Coyer,[‡] M. Croft,[§] J. Chen,[§] and R. H. Herber*,[‡]

Received September 12, 1991

The structure and bonding in two forms of the bisthiocyanate complex of Pt(II), $Pt[(bpy)(X)_2]$ (where bpy is 2,2′-bipyridyl and X is the pseudohalide), have been studied by solution and solid-state NMR, FTIR, and EXAFS spectroscopies. The yellow complex, which is soluble in a variety of organic solvents, contains two cis S-bonded SCN ligands and is the kinetically favored form. On heating, either in solution or as a solid, this complex transforms to a red insoluble complex, in which the SCN ligands have "flipped" to become N-bonded and which appears to be the thermodynamically stable form at room temperature. Conversion of the solid does not involve loss of a solvent molecule. EXAFS experiments involving the Pt-L_3 edge show the presence of two Pt–Pt distances in the red solid, one of which is indicative of the formation of stacked square planar Pt moieties, in which the 18-electron rule is satisfied.

The majority of known complexes of Pt(II), a d^8 transition metal, involve Pt sp^2d hybridization, giving rise to a square planar coordination of the ligands around the metal center. Such complexes display a rich (and challenging) set of chemical and physical properties, including various types of isomerism,[1] polychromism,[2] optical properties,[3] and a tendency to form chain-type polymers with anisotropic transport properties.[4] In addition, their importance as antineoplastic chemotherapeutic agents[5] have made these complexes the subject of intense study in recent years.

In particular, the thiocyanate complexes of Pt(II) have aroused considerable attention because of their unusual chemical and physical properties and have been the subject of several recent reviews.[6,7] The bisthiocyanate complexes of Pt(II), in which two coordination sites are occupied by a bidentate ligand, thus forcing the pseudohalide ligands to occupy cis positions, are of particular interest. Subtle chemical modifications of the bidentate ligand can be used to influence the nature of the pseudohalide bonding and the solvation of the solids, as well as the chemical properties of the product. In his extensive review of "ambidentate ligands", Burmeister[7] points out that there are, in fact, 10 distinguishable modes in which the SCN group can bond to a metal center, including ionic, simple covalent, bridging, linear, and bent bond formation. Of these, the M–SCN (type 13) and M–NCS (type 12) ligations are most fundamental in understanding the interaction between Pt and the "soft" (more easily polarizable, i.e., S) and "hard" (i.e., N) end of the ligand as it exists in a particular complex.

In this context, it was reported some time ago[8] that the bisthiocyanate complex of Pt(bipy) (where bipy is 2,2′-bipyridyl) can exist in two isomeric forms: a yellow complex which is soluble in a variety of (coordinating) solvents and which transforms under relatively mild conditions to a polymeric (red) species, which is insoluble and stable under ordinary conditions. As has been discussed by Kukushkin et al.[8] the two forms have the same stoichiometry, but their chemical and optical properties are distinctly different. This difference has been ascribed to several possible factors, including solvation,[2] polymerization, and ligand isomerization.[8] The latter possibility and its spectroscopic consequences have been discussed in detail by Burmeister,[7a] and an X-ray diffraction study of both S- and N-bonded thiocyanate complexes of palladium (1,1,7,7-tetraethyl)diethylenetriamine salts with tetraphenyl borate anions has been reported by Brock et al.[7b] However, to date (to the best of our knowledge) no single-crystal X-ray diffraction data have been reported which give unambiguous evidence for the ligand "flip" in Pt(II) complexes, which must

‡ Department of Chemistry.
§ Department of Physics.

(1) Engelter, C.; Thornton, D. A. *J. Mol. Struct.* **1977**, *42*, 51; Clark, R. J. H.; Williams, C. S. *Spectrochim. Acta* **1966**, *22*, 1081; Thompson, L. K. *Inorg. Chem.* **1980**, *38*, 117.
(2) Bielli, E.; Gidney, R. D.; Gillard, R. D.; Heaton, B. T. *J. Chem. Soc., Dalton Trans.* **1974**, 2133.
(3) Biedermann, J.; Wallfahrer, M.; Gliemann, G. In *Photochemistry and Photophysics of Coordination Compounds*; Yersin, H., Vogler, A., Eds.; Springer Verlag: Berlin, 1987.
(4) Williams, J. M. *Adv. Inorg. Chem. Radiochem.* **1983**, *25*, 235.
(5) Lippert, B. In *Progress in Inorg. Chem.*; Lippard, S. J., Ed.; Wiley and Sons: New York, 1989; Vol. 37; Lippard, J. J. *Pure Appl. Chem.* **1987**, *59*, 731; Reedijk, J. *Pure Appl. Chem.* **1987**, *59*, 181; Bednarski, P. J.; Ehrensperger, E.; Schoenberger, H.; Burgemeister, T. *Inorg. Chem.* **1991**, *30*, 3015 and references therein; Farrell, N. *Transition Metal Complexes as Drugs and Chemotherapeutic Agents*; Kluver Academic Publishing Co.: Dordrecht, The Netherlands, 1989; p 67; Gill, D. S. In *Platinum Compounds in Cancer Chemotherapy*; Hacker, M. P., Douple, E. B., Krakoff, I. H., Eds.; Martinus Nijhoff Pub. Co.: Boston, 1984.
(6) Burmeister, J. L. *Coord. Chem. Rev.* **1968**, *3*, 225; Basolo, F. *Coord. Chem. Rev.* **1990**, *100*, 47.
(7) (a) Burmeister, J. L. *Coord. Chem. Rev.* **1990**, *105*, 77. (b) Brock, C. P.; Huckaby, J. L.; Attig, T. G. *Acta Crystallogr.* **1984**, *B40*, 595.
(8) Kukushkin, Yu. N.; Vrublevskaya, L. V.; Vlasova, R. A.; Isachkina, T. S.; Postnikova, E. S.; Sheleshkova, N. K. *Zh. Neorg. Khim.* **1985**, *30*, 401; *Russ. J. Inorg. Chem.* (Engl. Transl.) **1985**, *30*, 224.

0020-1669/92/1331-1752$03.00/0